Title

TIME-RESOLVED VUV SPECTROSCOPY USING SYNCHROTRON RADIATION. II. ZEEMAN BEATS IN RESONANCE FLUORESCENCE OF THE 3p1 STATES IN KRYPTON AND XENON

Author

Matthias, E.

Publication Date

1977-07-01

Submitted to Chemical Physics Letters

LBL-6651 Preprint

TIME-RESOLVED VUV SPECTROSCOPY USING SYNCHROTRON RADIATION. II. ZEEMAN BEATS IN RESONANCE FLUORESCENCE OF THE $^3P_1$ STATES IN KRYPTON AND XENON

E. Matthias, M. G. White, E. D. Poliakoff,
R. A. Rosenberg, S.-T. Lee, and D. A. Shirley

July 1977

Prepared for the U. S. Department of Energy
under Contract W-7405-ENG-48

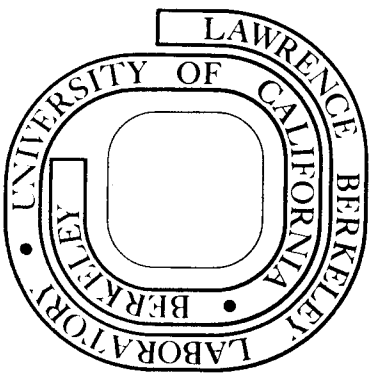

DISCLAIMER

TIME-RESOLVED VUV SPECTROSCOPY USING SYNCHROTRON RADIATION. II. ZEEMAN BEATS IN RESONANCE FLUORESCENCE OF THE $^3P_1$ STATES IN KRYPTON AND XENON*

E. Matthias,† M. G. White, E. D. Poliakoff, R. A. Rosenberg, S.-T. Lee,‡ and D. A. Shirley

Materials and Molecular Research Division
Lawrence Berkeley Laboratory
and
Department of Chemistry
University of California
Berkeley, California 94720

July 1977

ABSTRACT

Oriented states of atomic krypton and xenon have been produced and found to exhibit quantum beats in fluorescence, using pulsed vacuum-ultraviolet synchrotron radiation. This experiment demonstrates for the first time the feasibility of studying a number of atomic and molecular properties using synchrotron radiation, in direct analogy with in-beam accelerator based angular distribution studies of nuclei.

I. INTRODUCTION

Directional correlation of radiations was treated by Hamilton in 1940,[1] and perturbations of correlations by electromagnetic fields were discussed by Goertzel in 1946.[2] Since the first successful observation of gamma-ray angular correlations in nuclear decay by Brady and Deutsch in 1947,[3] a great deal of information about nuclear structure has been obtained from angular correlation studies, which yield spins and multipolarities, and from perturbed angular correlations, which yield electromagnetic moments.[4] In recent years nuclear spectroscopy has shifted from laboratory studies of decay schemes to accelerator-based work with systems created by nuclear reactions.[5] For these "in-beam" experiments, the beam axis substitutes for the first radiation, and time-dependent correlations are detected by pulsing the beam and measuring fluorescent radiation in coincidence.

In this Letter we point out that the availability of time-structured synchrotron radiation, together with fast timing and single photon counting techniques, makes "in-beam" studies of angular correlations and perturbed angular correlations possible for atomic and molecular systems at energies from the vacuum ultraviolet and beyond. Both the repetition rate and the photon energy available with synchrotron radiation far exceeds the present capability of UV lasers. We report the first perturbed angular correlation experiment based on synchrotron radiation, performed as a test of the feasibility of this technique. Finally, we conclude that spins, multipolarities, and electromagnetic moments, as well as dynamic properties, should be accessible to study by in-beam methods in atomic and molecular systems.

Quantum interference measurements in the vacuum ultraviolet (VUV) have been severely limited in the past for lack of narrow pulse, tuneable

light sources in this energy region. The continuously variable photon energy and excellent time structure (0.4 nsec pulse width, 780 nsec repetition rate) of the synchrotron radiation produced at the Stanford Positron Electron Accelerator Ring (SPEAR) is ideally suited for such experiments. Utilizing these time characteristics, energy separations from a few MHz to about 1 GHz can be measured. In the experiments reported here, a short VUV photon pulse coherently excited the magnetic sublevels of the $np^5(n+1)s^1\ ^3P_1$ excited state of a rare-gas atom. The subsequent fluorescence decay to the ^1S ground state was modulated at twice the Zeeman frequency.

II. THEORY

Two conditions must be met to produce an anisotropic angular distribution of radiation: an oriented state must be formed, and it must decay anisotropically. The first condition requires $J_{ex} \geqslant 1$. The second condition is usually satisfied for radiation of a single multipolarity, though with an anisotropy amplitude that depends on J_{ex} and J_{gr}.[4] If $\vec{k}_1$ and $\vec{k}_2$ represent the beam and detector directions, respectively, the intensity of fluorescent light observed at time t after excitation can be written[6]

$$W(\vec{k}_1,\vec{k}_2,t) = \mathrm{Tr}[\rho(\vec{k}_1,t)\varepsilon(\vec{k}_2)] \quad . \tag{1}$$

Here, $\rho(\vec{k}_1,t)$ is the density matrix describing the ensemble of excited states, and the efficiency matrix $\varepsilon(\vec{k}_2)$ characterizes the detector system. In terms of statistical tensors ρ^{λ}_{q}, $\varepsilon^{\lambda}_{q}$, Eq. (1) can be written

$$W(\vec{k}_1,\vec{k}_2,t) = \sum_{q,\lambda} \rho_q^{\lambda}(t)^*_{\vec{k}_1} \cdot \varepsilon_q^{\lambda}(\vec{k}_2) \quad . \tag{2}$$

Synchrotron radiation is linearly polarized and resonance absorption prepares the excited ensemble in a strongly oriented (polarization and alignment) state, which means ρ_q^{λ} has no rotational symmetry about $\vec{k}_1$ at t = 0. If the detector system is polarization sensitive, the same statement applies to ε_q^{λ} with respect to $\vec{k}_2$. In the experiments reported below, however, the detectors were not sensitive to linear polarization and hence the efficiency tensor was rotationally symmetric about $\vec{k}_2$. This implies that only terms with q = 0 contribute and Eq. (2) simplifies accordingly. Since only dipole radiation contributes, λ will be restricted to 0 and 2. The general expression for the angular correlation intensity becomes

$$W(\Theta,t) = A_0 e^{-t/\tau} [1 + A_2 P_2(\cos\Theta)] \tag{3}$$

where Θ is the angle between $\vec{k}_1$ and $\vec{k}_2$ and τ is the excited-state lifetime. For $J_{gr} = 0$, $J_{ex} = 1$, A_2 has the value 1/2.

Application of a magnetic field (z-axis) perpendicular to $\vec{k}_2$ (see Fig. 1) mixes the states with respect to this representation and the density tensor becomes time-dependent:

$$\rho_0^{\lambda}(t)^*_{\vec{k}_1} = \sum_{q,\lambda} \rho_{q'}^{\lambda}(0)^*_{\vec{z}} \cdot e^{-iq'\omega_0 t} \cdot D^{(\lambda)*}_{q'0}(\vec{z} \to \vec{k}_1) \quad , \tag{4}$$

where $\omega_0 = g_J \mu_B H_0/\hbar$ is the (Larmor) interaction frequency. Transformation of the representation from $\vec{k}_1$ into the $\vec{z}$-axis is described by the rotation group $D^{(\lambda)}_{0q'}(\vec{k}_1 \to \vec{z})$. A detailed calculation[4] of Eqs. (2) and

(4) leads to a simple periodic modulation of the fluorescence intensity

$$W(\Theta,t) = A_0\, e^{-t/\tau}\, [1 + A_2 P_2\, (\cos(\Theta-\omega_0 t))] \quad . \tag{5}$$

Direct observation of this modulation in fluorescent decay is possible if two additional conditions are satisfied. The substates must be coherently populated (in time) to insure a well defined phase relation in their time evolution (this in turn requires short light pulses, of width $T < \omega_0^{-1}$). Also, the level splitting must not be energetically resolved by the detectors.

III. EXPERIMENTAL

The experimental geometry is shown in Fig. 1. A detailed description of the gas cell and detection apparatus will be given elsewhere.[7] Briefly, monochromatized synchrotron radiation enters a gas flow cell through a LiF window isolating the SPEAR vacuum. The fluorescence decay curves were generated using standard single photon counting (with an EMR 541-G photomultiplier) and photon coincidence techniques which measure the time interval between the excitation pulse and a single fluorescence photon event. Sample pressures were kept in the $2\text{-}5 \times 10^{-6}$ torr range to avoid resonance radiation trapping, which would cause a dephasing between the fluorescence event and its detection, washing out the time modulation. Counting rates, exclusive of Rayleigh scattering events, were 15-20 sec^{-1}, necessitating accumulation times of 2-3 hours.

The external magnetic field was produced by an air-cooled Helmholtz coil pair around the gas cell, yielding field strengths up to 40 gauss. The application of larger external fields was precluded by the 1.8 nsec time

resolution of the detection apparatus.

IV. RESULTS

Figures 2 and 3 show the modulated decays of the $^3P_1$ states of Kr and Xe, respectively, for two magnetic field strengths. The large peak centered near t=0 (channel 760) arises from Rayleigh scattering events and its shape reflects the response function of the detector. The increase in modulation frequency with increasing magnetic field strength is clearly seen. The large difference in apparent modulation amplitude in Kr and Xe is a result of the hyperfine interaction in the abundant isotopes ^{129}Xe and ^{131}Xe. Table I lists the abundances and expected Zeeman frequencies for the various isotopes of Kr and Xe. Of course all even-even isotopes of each element have the same frequency in an external field. For Kr this includes 88.5% of all isotopes but in Xe only 52.4%. In addition, the Zeeman beat frequencies of the hyperfine components in ^{83}Kr are small compared to the dominant frequency. For Xe, however, the Zeeman frequencies of the hyperfine levels in ^{129}Xe and ^{131}Xe are comparable to or larger than the g_J-frequency in the J = 1 state of the even-even isotopes. This superposition of frequencies in Xe attenuates the modulation amplitude as shown in Fig. 3. In contrast, Kr exhibits one dominant frequency.

To extract the observed lifetimes and Zeeman beat frequencies, the modulated decay curves were fitted to Eq. (5), but with the detector response function and chance coincidence background taken into account. The results of the least-squares fit for the Zeeman beat frequencies and A_2 values are given in Table I. The A_2 values have been corrected for the finite solid angle of acceptance and for even isotope abundance. In

most cases, the derived frequencies and A_2 values agree within our experimental errors with the calculated values based on the g_J factors given in Moore's compilation[8] and the theoretical A_2 value of 1/2, respectively. The derived A_2 value for Kr at H_0 = 34G differs from the theoretical value by more than the assigned error. Because the other three values show excellent agreement with theory, we do not regard this disagreement as being significant. In addition, the derived lifetimes of 3.0 and 3.7 nsec for the 5s[3/2] J = 1 state of Kr and 6s[3/2] J = 1 state of Xe, respectively are in reasonably good agreement with those obtained at similar pressures in a previous study.[7]

V. DISCUSSION

In this work we have demonstrated for the first time the feasibility of producing oriented atomic states (angular correlations) and of observing quantum coherence effects in their decay (perturbed angular correlations), using pulsed synchrotron radiation. The technical problems of fast timing and of obtaining sufficient fluorescent intensity at low enough pressures to preserve coherence have been solved. Detectors with faster time response, such as channel plates, would facilitate the measurement of quantum beats with considerably higher accuracy. The formalism used for in-beam experiments in nuclear spectroscopy has been shown to predict our observed results.

It should now be feasible to employ synchrotron radiation at energies up through the VUV range and beyond to selectively populate excited states in atoms and molecules and observe their fluorescent decay. This will provide a general method for measuring lifetimes, spins (through A_2), and multipolarities if different from dipole, through higher-order terms.

As in nuclear spectroscopy, it will be possible to determine g_J factors even when the substates are unresolved in energy. Atomic and molecular excited-state quadrupole moments are also accessible, extending the recent Stark quantum beat studies with lasers[9] to the VUV range, in analogy with nuclear quadrupole-moment determinations by perturbed angular correlations.[4] Finally, dynamic processes such as gas-phase rotational relaxation can be studied through the apparent decay of the A_2 coefficient, in analogy with previous nuclear studies.[10]

REFERENCES

*This work was done with support from the U. S. Energy Research and Development Administration.
†Permanent address: Freie Universitat Berlin, Berlin, W. Germany
‡Permanent address: Eastman Kodak Research Labs., Rochester, New York.

1. D. R. Hamilton, Phys. Rev. 58, 122 (1940).

2. G. Guertzel, Phys. Rev. 70, 897 (1946).

3. E. L. Brady and M. Deutsch, Phys. Rev. 72, 870 (1947).

4. See for example, H. Frauenfelder and R. M. Steffen in Alpha-, Beta- and Gamma-Ray Spectroscopy, edited by K. Siegbahn (North-Holland publishing Co., Amsterdam, 1966), Vol. 3, p. 997.

5. E. Recknagel, in Nuclear Spectroscopy and Reactions, Part C, edited by J. Cerny (Academic Press, 1974), p. 93.

6. E. Matthias, B. Olsen, D. A. Shirley, J. E. Templeton, and R. M. Steffen, Phys. Rev. A4, 1626 (1971).

7. E. Matthias, S.-T. Lee, R. A. Rosenberg, E. D. Poliakoff, M. G. White, and D. A. Shirley, Chem. Phys. Lett., submitted for publication.

8. C. E. Moore, Atomic Energy Levels, U. S. Natl. Bur. of Stand. Circ. No. 467, (U.S. GPO, Washington, DC, 1962), Vols. 2 and 3.

9. A. Hese, A. Renn, and H. S. Schweda, Optics Commun. 20, 385 (1977).

10. D. A. Shirley and H. Haase, Ann. Rev. Phys. Chem. 23, 385 (1972).

TABLE I. Zeeman Frequencies in Krypton and Xenon

Kr ISOTOPES	abundance (%)	angular momentum	g-factor[a]	Zeeman frequency (MHz) H_0 = 34G	Zeeman frequency (MHz) H_0 = 27G	expt. (MHz) H_0 = 34G	expt. (MHz) H_0 = 27G	A_2[b] H_0 = 34G	A_2[b] H_0 = 27G
78, 80, 82, 84, 86	88.5	J = 1	1.242	59.10	46.93				
83	11.5	$F = \frac{11}{2}$	0.226	10.75	8.54	59.4(9)	47.0(5)	0.60(6)	0.52(5)
		$F = \frac{9}{2}$	0.050	2.38	1.89				
		$F = \frac{7}{2}$	-0.276	13.13	10.43				
Xe ISOTOPES									
124, 126, 128, 130, 132, 134, 136	52.39	J = 1	1.204	57.29	45.50				
129	26.4	$F = \frac{3}{2}$	0.803	38.20	30.34				
		$F = \frac{1}{2}$	1.605	76.39	60.66	57.9(7)	45.9(7)	0.51(5)	0.47(5)
131	21.2	$F = \frac{5}{2}$	0.482	22.92	18.20				
		$F = \frac{3}{2}$	0.321	15.28	12.13				
		$F = \frac{1}{2}$	-0.80	38.20	30.34				

a) Reference 8.

b) Experimental A_2 values corrected for isotope abundance and finite solid angle. Geometrical considerations including a line source yield an approximate solid angle correction of 0.89 ± .03.

FIGURE CAPTIONS

Fig. 1 Experimental geometry.

Fig. 2 Zeeman beat measurements for the Kr 5s[3/2]1 state. Dots are real data points with backround subtracted. The lines represent the least-squares fit to equation (5). Note that the fits do not include the prompt response function (centered at channel number 775) and begin at channel numbers 675 and 700 for the low and high field measurements, respectively.

Fig. 3 Zeeman beat measurements for the Xe 6s[3/2]1 state. Dots are real data points with backround subtracted. The lines represent the least-squares fit to equation (5). Note that the fits do not include the prompt response function (centered at channel number 783) and begin at channel numbers 686 and 707 for the low and high field measurements, respectively.

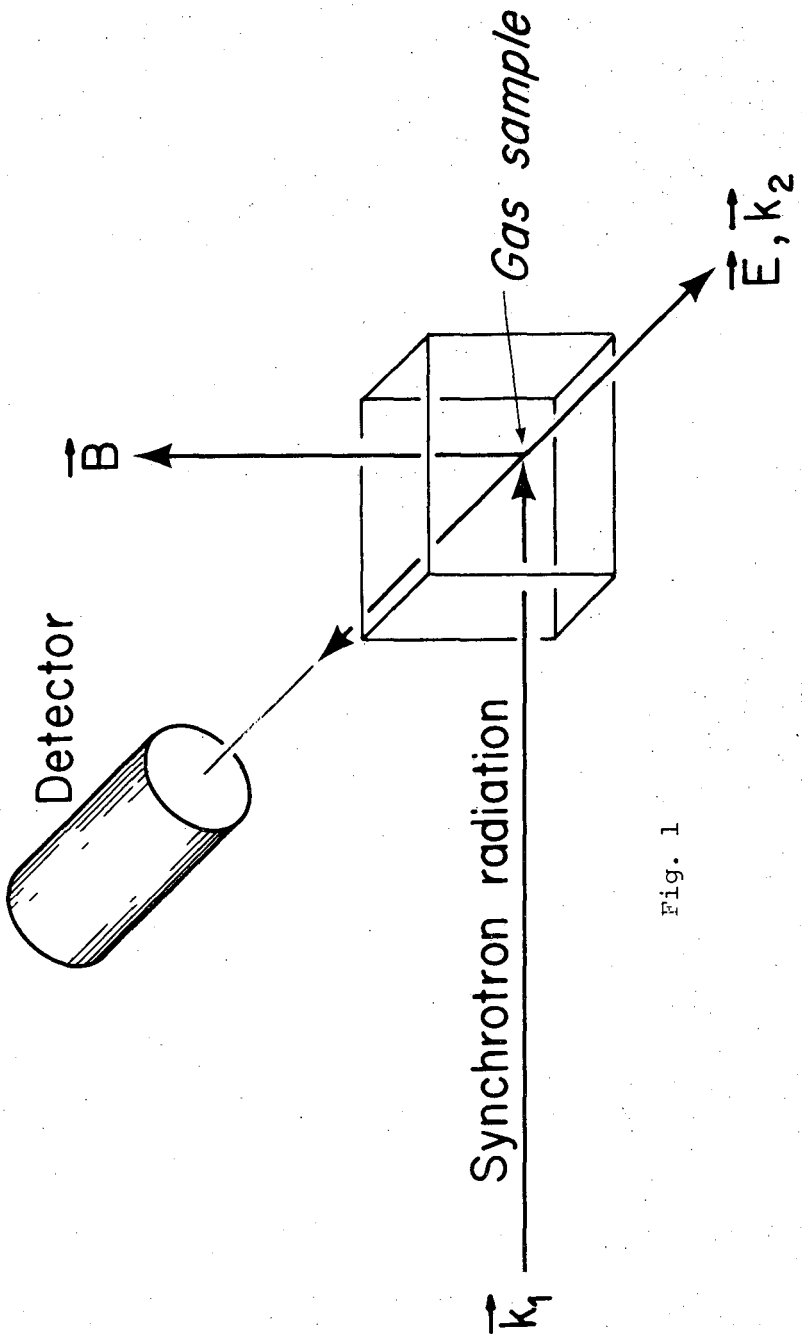

XBL 779-1950

Fig. 1

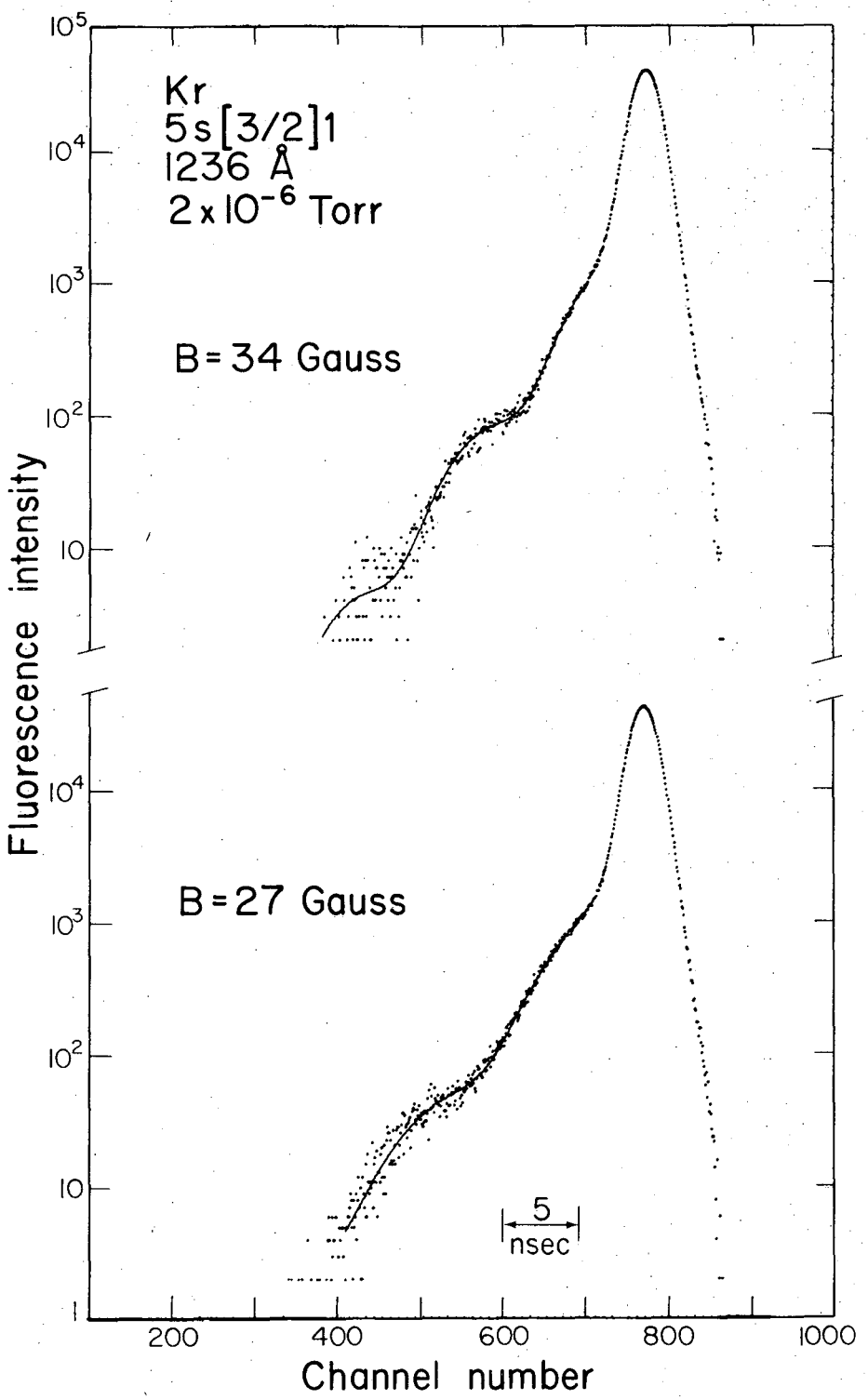

Fig. 2

XBL 779-1949

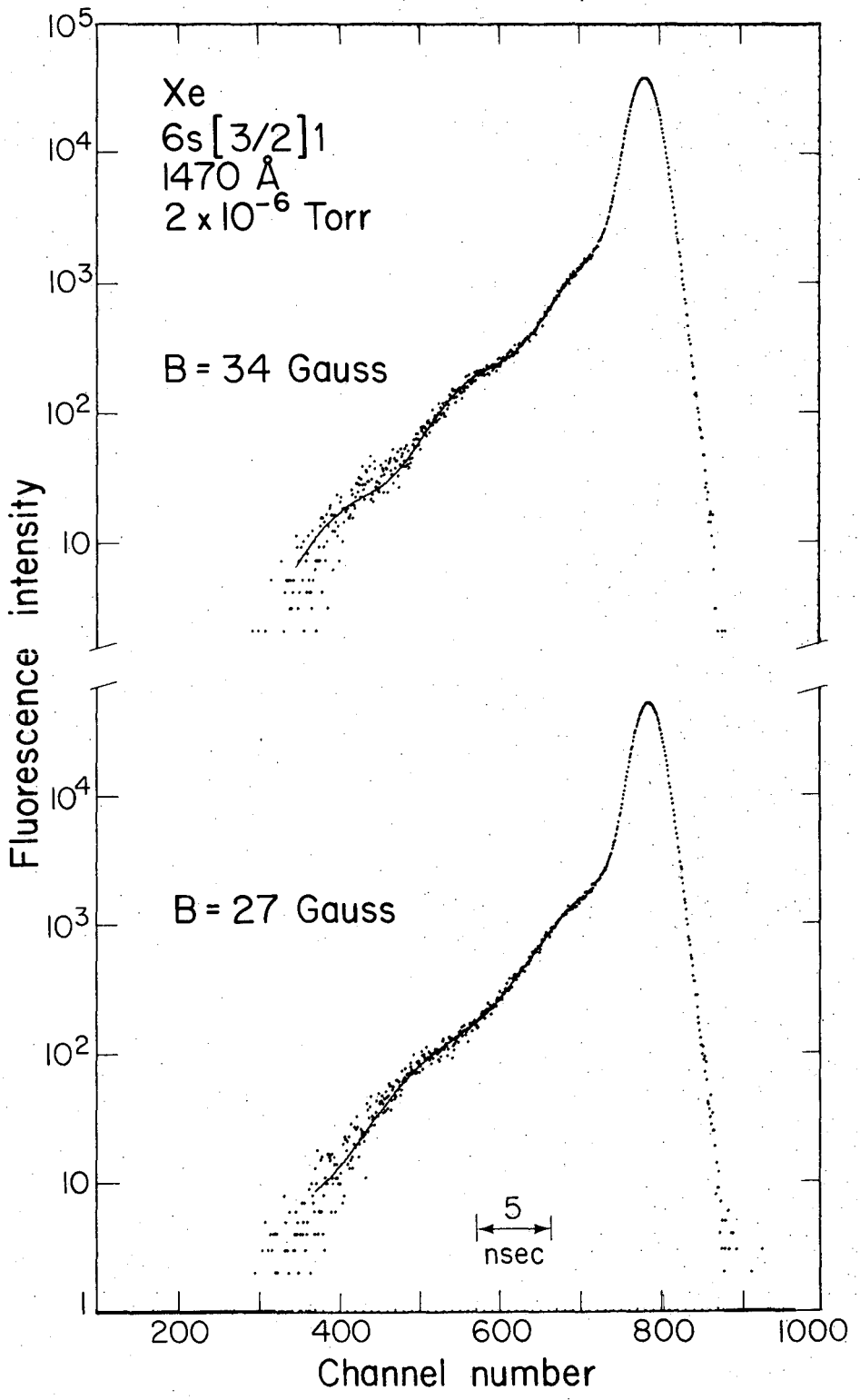

XBL 779-1948

Fig. 3

TECHNICAL INFORMATION DEPARTMENT
LAWRENCE BERKELEY LABORATORY
UNIVERSITY OF CALIFORNIA
BERKELEY, CALIFORNIA 94720